Protein Science (1994), *3*:1760–1769. Cambridge University Press. Printed in the USA.

Structure–function relationship in the globular type III antifreeze protein: Identification of a cluster of surface residues required for binding to ice

HEMAN CHAO,[1] FRANK D. SÖNNICHSEN,[2] CARL I. DELUCA,[1] BRIAN D. SYKES,[2] AND PETER L. DAVIES[1]

[1] Department of Biochemistry, Queen's University, Kingston, Ontario K7L 3N6, Canada
[2] Protein Engineering Network of Centres of Excellence and Department of Biochemistry, University of Alberta, Edmonton, Alberta T6G 2S2, Canada

(RECEIVED July 14, 1994; ACCEPTED August 2, 1994)

Abstract

Antifreeze proteins (AFPs) depress the freezing point of aqueous solutions by binding to and inhibiting the growth of ice. Whereas the ice-binding surface of some fish AFPs is suggested by their linear, repetitive, hydrogen bonding motifs, the 66-amino-acid-long Type III AFP has a compact, globular fold without any obvious periodicity. In the structure, 9 β-strands are paired to form 2 triple-stranded antiparallel sheets and 1 double-stranded antiparallel sheet, with the 2 triple sheets arranged as an orthogonal β-sandwich (Sönnichsen FD, Sykes BD, Chao H, Davies PL, 1993, *Science 259*:1154–1157). Based on its structure and an alignment of Type III AFP isoform sequences, a cluster of conserved, polar, surface-accessible amino acids (N14, T18, Q44, and N46) was noted on and around the triple-stranded sheet near the C-terminus. At 3 of these sites, mutations that switched amide and hydroxyl groups caused a large decrease in antifreeze activity, but amide to carboxylic acid changes produced AFPs that were fully active at pH 3 and pH 6. This is consistent with the observation that Type III AFP is optimally active from pH 2 to pH 11. At a concentration of 1 mg/mL, Q44T, N14S, and T18N had 50%, 25%, and 10% of the activity of wild-type antifreeze, respectively. The effects of the mutations were cumulative, such that the double mutant N14S/Q44T had 10% of the wild-type activity and the triple mutant N14S/T18N/Q44T had no activity. All mutants with reduced activity were shown to be correctly folded by NMR spectroscopy. Moreover, a complete characterization of the triple mutant by 2-dimensional NMR spectroscopy indicated that the individual and combined mutations did not significantly alter the structure of these proteins. These results suggest that the C-terminal β-sheet of Type III AFP is primarily responsible for antifreeze activity, and they identify N14, T18, and Q44 as key residues for the AFP–ice interaction.

Keywords: NMR; site-directed mutagenesis; thermal hysteresis

Some cold water marine fishes produce proteins or glycoproteins that lower the freezing point of their blood without significantly increasing its osmolarity (DeVries, 1983; Davies & Hew, 1990). These antifreeze proteins or glycoproteins bind to and halt the growth of seed ice crystals that form in solution at or below the equilibrium freezing point (Raymond & DeVries, 1977). As the solution is cooled further, there comes a point where ice crystal growth is reinitiated. The difference in temperature between this nonequilibrium freezing point and the melting temperature is referred to as thermal hysteresis, the magnitude of which is a function of AFP concentration. DeVries and Lin (1977) and DeVries (1984) suggested that these antifreezes stop ice growth by adsorbing to specific ice planes via hydrogen bonds. This hypothesis remains central to all models proposed so far for antifreeze action.

At present, the best characterized fish antifreeze proteins are the Type I AFPs. In winter flounder, these are small (M_r 3,000–4,000) alanine-rich, α-helical peptides that have regularly spaced

Reprint requests to: Peter L. Davies, Department of Biochemistry, Queen's University, Kingston, Ontario K7L 3N6, Canada.

Abbreviations: AFGP, antifreeze glycoprotein; AFP, antifreeze protein; FPLC, fast protein liquid chromatography; H bond, hydrogen bond; NOESY, nuclear Overhauser effect spectroscopy; QAE, quaternary aminoethyl/AFP isoform that binds QAE-Sephadex; TOCSY, total correlation spectroscopy; 1D, one-dimensional; 2D, two-dimensional; 3D, three-dimensional.

threonines and asparagines (or aspartic acid) on 1 side of the helix (Yang et al., 1988). Ice etching studies showed preferential adsorption of these peptides to the hexagonal bipyramidal planes {2021} with alignment in the ⟨0112⟩ direction (Knight et al., 1991). A match was found between the distance of repeating polar residues on the peptide (16.5 Å) and the spacing of oxygen atoms on the deduced ice plane (16.7 Å). This provided an attractive explanation for the mechanism of action based on the fit of H-bonding groups. The importance of strategically placed polar residues has been further supported by the study of Wen and Laursen (1992a), who showed that rearrangement of regularly spaced threonines and asparagines can result in loss of antifreeze activity.

AFGP is another long, linear, amphipathic molecule for which a model has been developed for its H bonding to a specific ice plane (Knight et al., 1993). In this model, disaccharides attached to tripeptide repeats form 2 H bonds to ice at regular intervals along the lattice.

In contrast to these 2 types of antifreeze proteins that have little or no tertiary structure, Type III AFP (M_r 7,000) is a compact, folded protein (Sönnichsen et al., 1993). It consists of 9 short β-strands and several turns. The strands are paired to form 2 triple-stranded, antiparallel sheets arranged as an orthogonal β-sandwich, and 1 double-stranded, antiparallel sheet (Chao et al., 1993). Unlike Type I AFP and the AFGPs, its globular fold and lack of obvious repetitive structure make it difficult to predict a match to the ice lattice.

To delineate which area of the protein interacts with ice and which amino acids play an important role in antifreeze activity, we targeted polar residues for mutagenesis. The effect of the mutations on protein activity was determined by thermal hysteresis measurements, and the integrity of the fold of all the mutants was confirmed by NMR spectroscopy. At positions where mutations had an effect, exchange between hydroxyl and amide side chains decreased antifreeze activity markedly, but the replacement of an amide by its carboxylic acid was a neutral change. From our analysis of 12 different mutant AFPs involving 5 residues, 3 functionally critical amino acids have been identified on the C-terminal β-sheet. Our results suggest there is a novel arrangement of ice-binding residues, which differs from that seen in Type I AFP or AFGP.

Results

Recombinant Type III AFP used for this study (rQAE m1.1) has been previously characterized (Chao et al., 1993). The sequence of this protein (Fig. 1) closely matches that of native QAE, 1 of at least 12 different isoforms isolated from serum of ocean pout, *Macrozoarces americanus*. Differences are an initiating methionine (Met 0) and a C-terminal sequence YAA (instead of YPPA). The latter mutation was required to suppress a *cis–trans* proline isomerization observed with the native QAE sequence. This mutant was used for structure elucidation by NMR spectroscopy and was shown to be indistinguishable from native QAE in its antifreeze activity (Sönnichsen et al., 1993). Thus, for simplicity we will refer to this recombinant protein (rQAE m1.1) as "wild type" throughout this paper. All mutations were derived from this mutant sequence to allow for a direct comparison of activity changes as well as the NMR spectroscopic characterization of the mutant proteins.

Effects of pH on antifreeze activity

The influence of pH on the activity of Type III AFP was studied to see if different ionization states of charged side chains affected the ability of AFP to bind to ice. For wild-type QAE, antifreeze activity was unchanged from pH 2 to pH 11 (Fig. 2). Even at the pH extremes of 1 and 13, the antifreeze activity was only decreased by 20% and 27%, respectively. This is a remarkably broad pH optimum for a protein activity. It indicates that the protein fold is stable over a wide pH range and agrees with observations by NMR spectroscopy that between pH 4.8 and

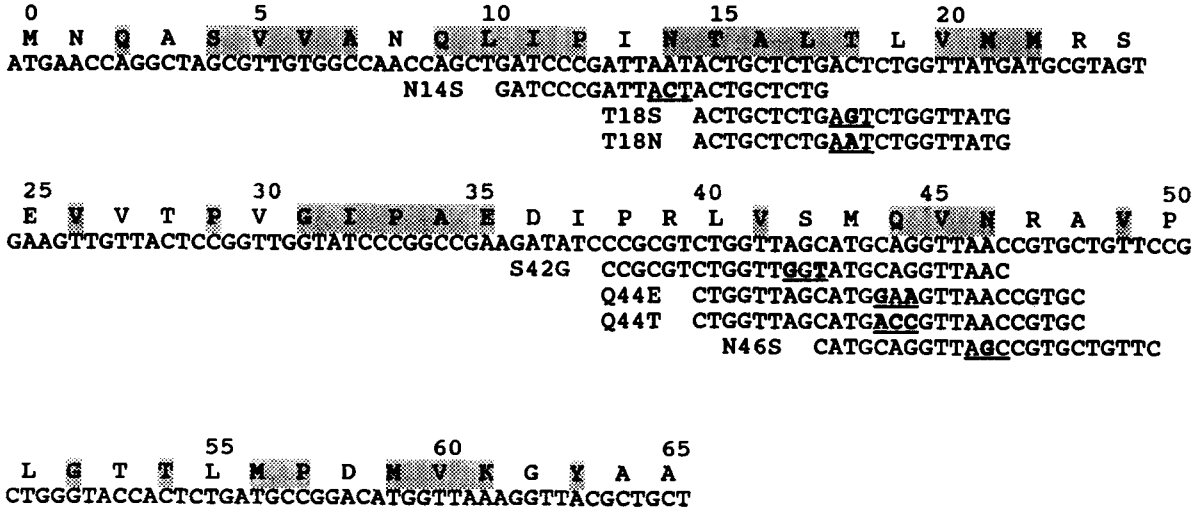

Fig. 1. List and alignment of mutagenic oligonucleotide sequences. The DNA sequence of each mutagenic oligonucleotide is presented with the codons effecting amino acid changes underlined and the altered bases in bold. The amino acid sequence of rQAE m1.1 is shown for comparison with the initiating methionine labeled as residue 0. Amino acids that are invariant in Type III AFP isoforms (Davies & Hew, 1990) are shaded.

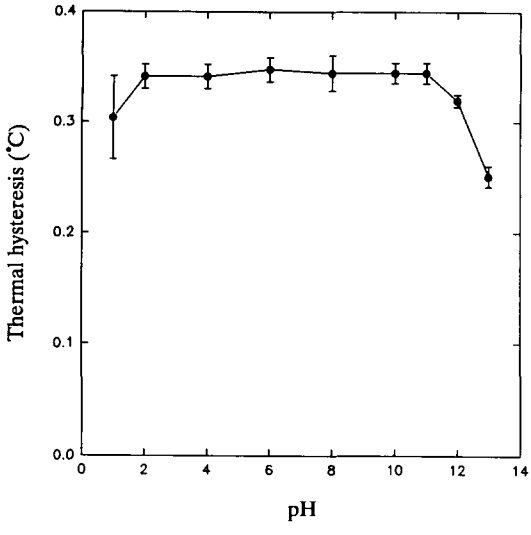

Fig. 2. The effect of pH on thermal hysteresis activity of Type III AFP. Thermal hysteresis activity of rQAE m1.1 (1.0 mg/mL) was measured at pH values ranging from 1 to 13 at intervals of 1 or 2 pH units as outlined in the Materials and methods. Each data point represents the mean of 3 determinations. Standard deviations are shown as vertical bars.

pH 8.0 no significant structural changes were detected (Sönnichsen et al., 1993).

Site-directed mutagenesis of residues on the C-terminal β-sheet

The globular structure of Type III AFPs is devoid of simple repetitive sequences, which has precluded a straightforward identification of interacting residues. Based on its 3D structure, we previously noted 2 surfaces on the protein that have a preponderance of hydrophilic residues and could, therefore, be candidates for ice-binding sites (Sönnichsen et al., 1993). These hydrophilic surfaces correspond most closely to the triple-stranded β-sheets on opposite sides of the protein. Of these 2 possibilities, the triple sheet including the C-terminal β-strand was considered to be the more likely ice-binding surface for the following reasons. This sheet is arranged in a more planar fashion and has a greater number of hydrophilic residues than the N-terminal β-sheet. Moreover, several of these residues are conserved in all known Type III AFP primary sequences (Chao et al., 1993). The latter is a powerful argument because the positioning of ice-binding residues must be fairly precise, otherwise ice-binding motifs would occur frequently in proteins. Therefore, we selected this face for mutational analysis beginning with single amino acid replacements. Because pH studies failed to identify a role for the ionization state of residues in antifreeze action, we targeted the conserved, neutral hydrophilic, surface-accessible amino acids of the C-terminal β-sheet for site-directed mutagenesis (Table 1; Fig. 3; Kinemage 1). Other polar residues were chosen as replacements at these sites in order not to compromise protein fold stability or other properties such as solubility.

Four completely conserved sites on or near the C-terminal β-sheet, N14, T18, Q44, and N46, were targeted for mutagenesis. Specific mutations at the first 3 sites led to greatly reduced thermal hysteresis activities when compared to wild-type QAE. Of

Table 1. *Mutations of the C-terminal β-sheet polar residues*

Residue	Surface accessibility[a]	Mutation(s)
N14	0.63	D,Q,S
T18	0.28	N,S,T
S42	0.61	G
Q44	0.56	E,T
N46	0.13	S

[a] Surface accessibility is the ratio between the calculated accessible surface area of a side chain in the NMR structure of Type III AFP (Chao et al., 1993) and the surface area of the side chain in random coil (Shrake & Rupley, 1973).

the mutants tested, T18N on β-strand 15–18 showed the greatest loss of thermal hysteresis activity. At 1 mg/mL (0.14 mM), T18N had only 10% of the wild-type activity (Fig. 4A). In contrast, the activity of mutant T18S was indistinguishable from that of the wild type at all concentrations tested (Fig. 4A).

Replacement of N14 (immediately before β-strand 15–18) with serine resulted in a significant drop in antifreeze activity. At 1 mg/mL, N14S had only 25% the activity of wild-type QAE (Fig. 4B). Lengthening the side chain by a methylene group in N14Q produced an antifreeze that was intermediate in activity (67%) between N14S and the wild type (Fig. 4B). N14D was constructed to probe the role of the amide group at this site. Rather surprisingly, this mutant was fully active not only at pH 6.0, but also at pH 3.0, where the carboxyl group should be mainly protonated (Table 2).

Evidence for the involvement of Q44 on β-strand 43–46 in ice-binding came from mutant Q44T, which at 1 mg/mL had less than 50% of the activity of wild-type QAE (Fig. 4C). Mutant Q44E was made to test the role of the amide group, without changing the length of the side chain. As was observed for N14D, Q44E was fully active at both pH 6 and pH 3 (Table 2).

N46 is another conserved polar residue located on β-strand 43–46 on the C-terminal β-sheet of Type III AFP. Inspection of the 3D structure showed that its polar side chain could lie near a plane defined by the side chains of N14, T18, and Q44 (Fig. 3; Kinemages 1, 2). Because the replacement of N14 by serine had significant effects on antifreeze activity, N46S was expected to be less active if the amide of N46 was an ice-binding group. However, N46S was fully active, suggesting that its side chain is not important for ice binding (Fig. 4D).

We also mutated S42, a nonconserved amino acid immediately before β-strand 43–46. Because glycine is present at this location in most other isoforms, the role of this residue might be to induce a turn in the peptide backbone. Nevertheless, because S42 is located close to the plane defined by the 3 critical residues N14, T18, and Q44, and because it is an uncharged polar residue, it was targeted for mutagenesis. Mutation to glycine was chosen to remove the capacity to H-bond while preserving the turn. Not too surprisingly, mutant S42G was fully active (Fig. 4D). It showed that the hydroxyl group of S42 is not important for wild-type QAE antifreeze action.

Double and triple mutants

The effect of combining mutations was cumulative. The double mutant N14S/Q44T was less active than N14S or Q44T. At

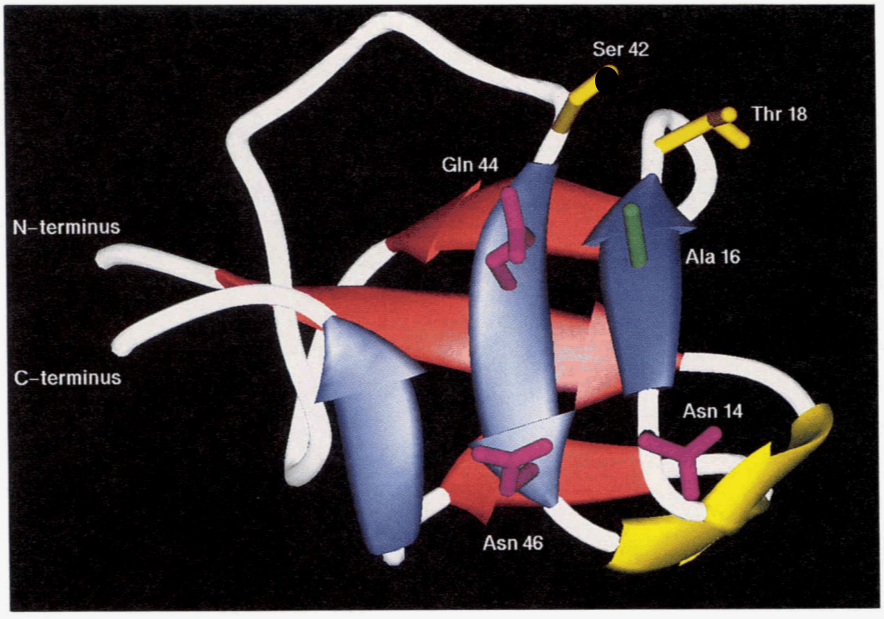

Fig. 3. Ribbon presentation of the globular Type III AFP showing the disposition of selected side chains on and around the C-terminal β-sheet. The N- and C-terminal β-sheets are colored red and blue, respectively. Side chains of selected residues are illustrated in a stick presentation, labeled with residue type and sequence number. The color code for the various residues is S and T, yellow; Q and N, purple; A, green.

1 mg/mL (Fig. 4C), it only had 10% of the activity of wild-type QAE compared to 25% for N14S and 47% for Q44T (Fig. 4B,C). Removal of 3 putative ice-binding groups (mutant N14S/T18N/Q44T) rendered the protein completely inactive (Fig. 4C).

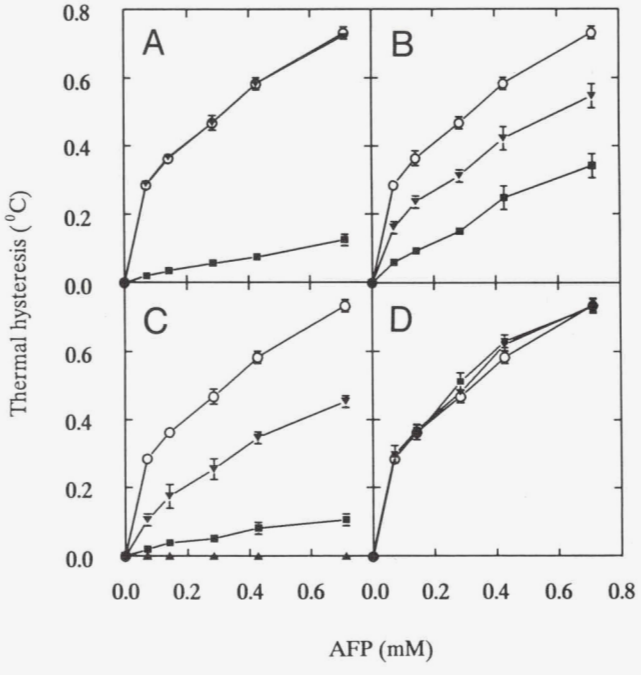

Fig. 4. Antifreeze activity of Type III AFP mutants. Thermal hysteresis values for Type III mutants and rQAE m1.1 at various concentrations were compared. Assays were performed in 0.1 M NH_4HCO_3 (pH 7.9). Each data point represents the mean of 3 determinations. Standard deviations are shown as vertical bars. **A:** Activity curves for rQAE m1.1 (○—○), T18S (▼—▼), and T18N (■—■). **B:** Activity curves for rQAE m1.1 (○—○), N14Q (▼—▼), and N14S (■—■). **C:** Activity curves for rQAE m1.1 (○—○), Q44T (▼—▼), N14S/Q44T (■—■), and N14S/T18N/Q44T (▲—▲). **D:** Activity curves for rQAE m1.1 (○—○), S42G (▼—▼), and N46S (■—■).

Confirmation of the protein fold

NMR spectroscopic studies were performed to confirm the integrity of the fold of all mutant Type III AFPs. Clearly, a change in tertiary structure could alter the mutant's activity without the possibility of determining the role of the mutated side chain in the protein–ice interaction. The triple mutant (N14S/T18N/Q44T) was chosen for complete characterization because establishing the correctness of its fold would strongly suggest that all encompassed single and double mutants were also correctly folded. 2D ^{1}H-NMR spectra of the triple mutant, as illustrated by the 2D NOESY analysis (Fig. 5), are very similar to those of the wild type (Chao et al., 1993). With a β-sandwich fold consisting of 2 antiparallel triple-stranded sheets and 1 antiparallel double-stranded sheet (Sönnichsen et al., 1993), $d_{\alpha\alpha}$ cross peaks between residues in neighboring strands were characteristic of the folded protein. Figure 5 clearly indicates that the expected $d_{\alpha\alpha}$ cross peaks were present in the triple mutant with similar intensity. The only differences between the spectra (apart from noise and signal loss at 5.02 ppm due to decoupling of the water) were the gain or loss of intraresidue connectivities stemming from the mutated residues (T18, T44), and the overlap of V45–V60 and

Table 2. *Effect of pH on the antifreeze activity of N14D and Q44E*

Sample (1.0 mg/mL)[a]	pH 3.0 (°C)[b]	pH 6.0 (°C)[b]
rQAE m1.1	0.35 ± 0.01	0.35 ± 0.02
N14D	0.37 ± 0.02	0.36 ± 0.02
Q44E	0.36 ± 0.02	0.37 ± 0.03

[a] The thermal hysteresis activities of N14D, Q44E, and the rQAE m1.1 standard at a concentration of 1 mg/mL were measured at pH 3.0 and pH 6.0 as described in the Materials and methods.

[b] Values in °C are the average of 3 determinations with standard deviations shown.

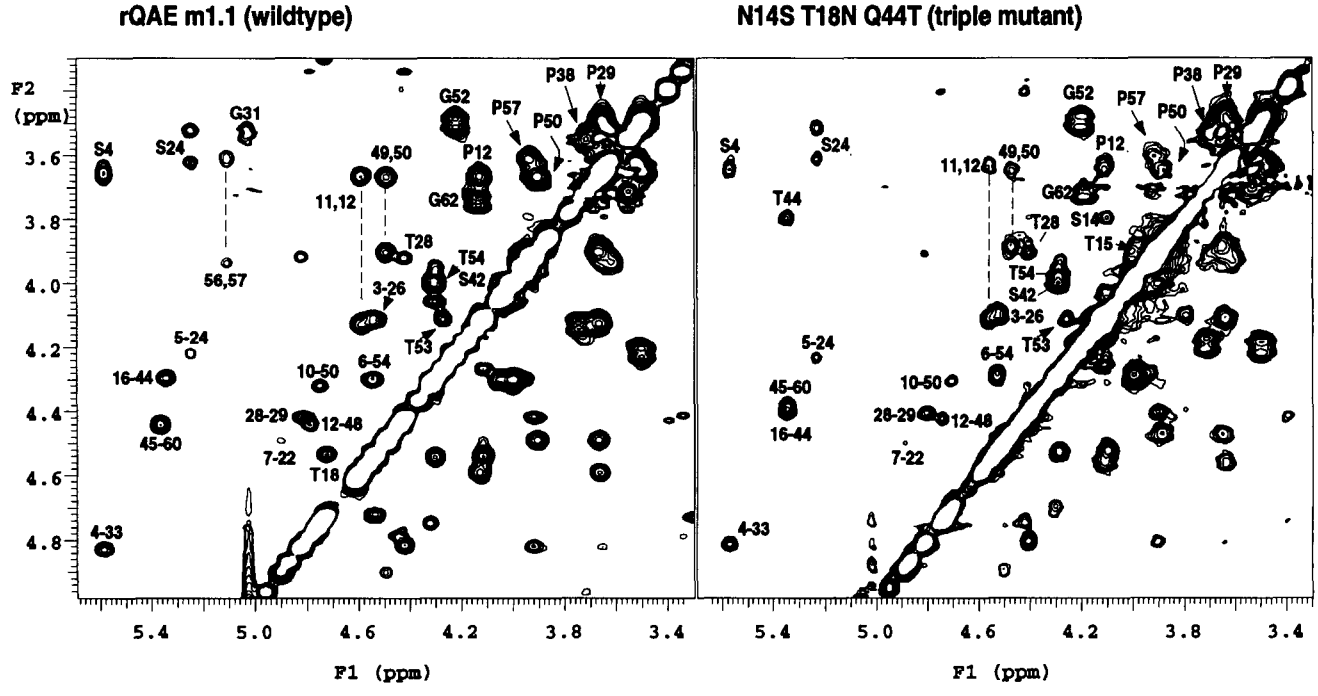

Fig. 5. Comparison of portions of 2D ^{1}H-1HH-NOESY NMR spectra containing characteristic $d_{\alpha\alpha}$ cross peaks for wild-type AFP (rQAE m1.1) and the triple mutant protein (N14S/T18N/Q44T). Cross peaks between αCH protons, indicative of the all-β-structure of the protein and of the *cis*-conformation of Pro 29, are labeled with the number of the residues involved separated by a dash. Intraresidue cross peaks are labeled with the 1-letter amino acid code and sequence number, and sequential connectivities involving Pro δCH ($d_{\alpha\delta(i,i+1)}$) are connected by vertical dashed lines and are marked with the residue numbers separated by a comma.

A16–T44 $d_{\alpha\alpha}$ cross peaks due to the shift of the A16 resonance in the triple mutant.

Chemical shifts are structurally sensitive NMR parameters; in particular, αCH shifts are strongly protein structure-dependent (Wishart et al., 1991). A complete comparison of αCH-chemical shifts in the wild type and in the triple mutant (Fig. 6) revealed that most residues were not affected by the mutations. Within the accuracy of the chemical-shift data ($\pm$0.02 ppm), the shifts were identical in the 2 proteins. Residues in close proximity to the mutations, either in or adjacent to the C-terminal triple sheet (13–20, 42–48, and 59–62), exhibited changes in αCH chemical-shift values of less than 0.1 ppm. The largest change was observed for A16 (0.11 ppm), which is surrounded by the 3 mutations. Given the range of structurally induced chemical-shift changes of αCH protons, these small changes establish that the mutation of N14, T18, and Q44 did not affect the structure of Type III AFP. As expected, larger deviations (>0.1 ppm) were observed only for the mutated residues.

One-dimensional ^{1}H-NMR spectra were acquired for all mutants at 3 °C and with D_2O as a solvent. These conditions have been shown to facilitate the observation of amide protons involved in the structurally characteristic H-bond network of wild-type AFP, whereas non-H-bonded protons exchange rapidly with the solvent and are therefore not observed (Chao et al., 1993). Figure 7 shows the spectra of the previously assigned wild-type QAE and all mutants of the C-terminal β-sheet region that had altered antifreeze activity. With the exception of the spectrum of the triple mutant (see below), all other spectra were quite similar. Amide proton resonance location and intensity were comparable for most residues, allowing their immediate assignment by comparison with the spectrum of the wild type. For mutants Q44T, and the triple mutant (as discussed above), these assignments were also confirmed by 2D TOCSY spectra. The observation of the same amide resonances under these conditions in all spectra indicated the preservation of the H bonding pattern within each protein and thus confirmed the integrity of

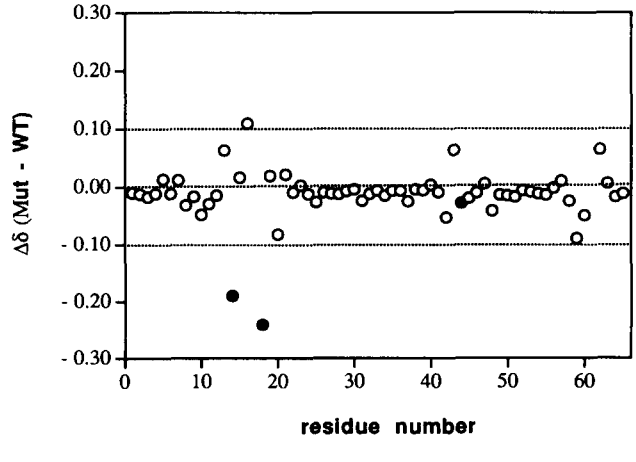

Fig. 6. NMR chemical-shift differences for αCH protons in fully active Type III (rQAE m1.1) and the triple mutant (N14S/T18N/Q44T). Open circles represent the chemical-shift differences between the 2 proteins for each residue ($\delta_{mutant} - \delta_{WT}$). For mutated residues (filled circles), the difference in secondary shifts for the αCH protons is also given ($\delta_{obs} - \delta_{rc}$) using random coil values from Wishart et al. (1991).

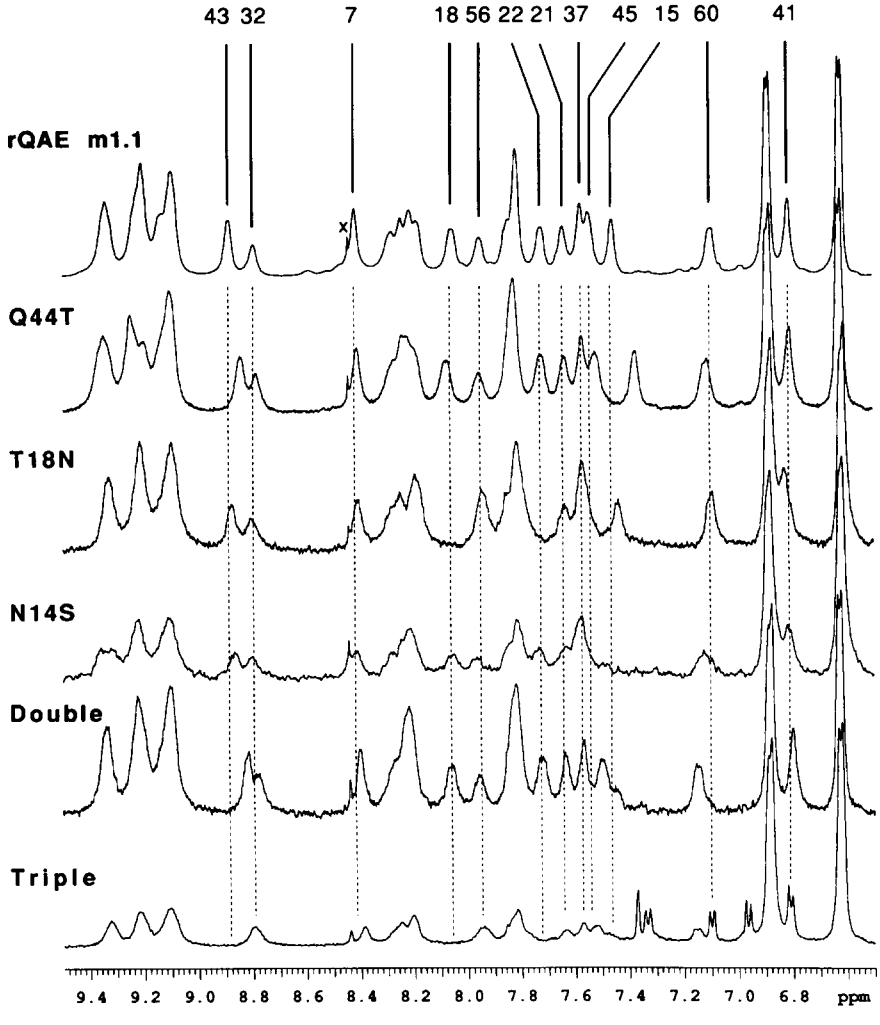

Fig. 7. Amide and aromatic region of 1D ^{1}H-NMR spectra of Type III AFP mutants. The spectra were acquired at 3 °C in D_2O at pH 7.0. Under these conditions, only slowly exchanging amide protons are observable >3 h after dissolving the proteins. Resolved resonances in the fully active Type III AFP (rQAE m1.1) are labeled with their sequence number. Vertical, dashed lines are used to reference amide resonance frequencies of rQAE m1.1 in the spectra of the activity mutants N14S, T18N, Q44T, N14S/T18N (double mutant), and N14S/T18N/Q44T (triple mutant). Impurities are marked (x).

their fold. Only small chemical-shift changes were observed for the amide resonance in these spectra and these were limited to the mutated residues or their immediate neighbors in sequence or space. The chemical-shift changes in the double and triple mutants were mostly consistent with the sum of the individual mutations. Judging by these data and by the 2D characterization of the triple mutant, it can be deduced that none of the mutant structures were significantly altered from that of the wild type.

The spectrum of the triple mutant (Fig. 7) differs in some aspects from that of the wild type. Several low-intensity doublets were present in the aromatic region that were not seen in other mutants. These additional Y63 resonances originated from 2 other isoforms of the protein present in this sample. Judged by the significantly smaller resonance line width and the lack of cross peaks of the minor forms in 2D NOESY spectra (Fig. 5), they represent partially unfolded forms of the protein. This was confirmed by a series of 1D spectra taken over 2 days (data not shown), which showed a decrease of signal intensity for the resonances of the folding intermediates (7.33 and 6.97 ppm; 710 and 6.81 ppm) while at the same time the intensity of the Y63 side-chain resonances in the folded protein (6.72 and 6.89 ppm) increased. This indicated that after protein purification, which involved denaturing conditions, the mutant had not refolded completely before being subjected to NMR analysis. Because this sample was refolded identically to all other AFP samples, the observation indicated changes in the mutant's folding kinetics, which will be worthy of future investigation. Also, the intensity of all amide resonances was significantly reduced compared with all other mutants and the wild type. This was partly due to the unfolded forms or folding intermediates present in this sample. However, it also reflects increased exchange rates of these core amides in the triple mutant. The amide exchange rates can be correlated with the local flexibility or stability (Kim & Woodward, 1993). However, the slowest exchange rates were still in the order of days as in the wild-type protein and thus, the changes in local protein flexibility are small. Taken together, both aspects could have slightly altered antifreeze activity, however, they cannnot be responsible for the complete loss of thermal hysteresis observed for the triple mutant.

Discussion

This study clearly identifies 3 residues in the C-terminal β-sheet, N14, T18, and Q44, as being primarily responsible for antifreeze activity (see Kinemages 1, 2). Structural alterations at these res-

idues, which are capable of H bonding with water molecules, reduce the antifreeze activity and may do so by disrupting an H bonding network that matches the ice lattice. The results suggest that H bond formation is an important factor for protein-ice adsorption, and that this interaction is very sensitive to the exact geometry of the H bonding groups, which implies that the AFP-ice interface is fairly rigid.

Comparison of the mutations of residues N14, T18, and Q44

Relatively conservative mutations from one polar, H bond-forming residue to another led to significant reductions in antifreeze activity of Type III AFP. The most detrimental mutation was T18N (10% active), followed by N14S (25%) and Q44T (50%). In all 3 mutations, the side-chain geometry as well as the nature of the polar group were altered. In mutant T18N, the side-chain length and side-chain volume were both increased, which could lead to steric disturbance of the protein-ice interface in addition to the weakening or loss of H bond(s) at the mutation site. A second explanation for the severity of this mutation uses suggestions by Knight et al. (1993), who proposed that ice-binding residues form part of the crystal lattice and thus can be involved in more than 1 H bond per group. In this proposal, hydroxyl groups of the sugar moieties in AFGP, or of threonyl and seryl residues in AFP, would be positioned at ice-crystal coordinates usually occupied by water molecules. Ideally, this allows for the formation of 3 H bonds in a tetrahedral coordination. Such a convenient coordination arrangement is not available for planar amide groups (Asn, Gln); consequently, modeling studies (Wen & Laursen, 1992b; Madura et al., 1994) indicate other preferred positions for these side chains. These differences in H bonding possibilities between the hydroxyl groups and amide groups might help explain the large reductions in activity shown by mutants N14S, T18N, and Q44T, where hydroxyl and amide groups have been exchanged. In line with this reasoning, Ser has a similar side-chain geometry to Thr and thus might occupy the same adsorption site. This is confirmed by the full activity of mutant T18S. It is also worthy of note that the expected additional flexibility of the Ser side chain seems not to have affected the ice-protein interaction. N14Q, another mutant with no change in the nature of the polar group, showed less than half the activity loss of N14S (67% compared to 25%). Whereas N14S introduces both a shortened side chain and a change in H bonding group, N14Q might be a less severe mutant because only the position of the polar group- or residue-specific ice-adsorption site has changed.

The role of charged groups

The thermal hysteresis activity of wild-type QAE is remarkably insensitive to the solution pH. Leaving aside the issue of the stability of the protein fold at different pH values, it is also of interest to consider the role of charged groups (if any) in binding to ice. For wild-type QAE, it is possible that charged groups are not involved simply because there are none appropriately positioned to contribute to the ice-binding surface of the AFP. Therefore, to explore the potential for charged groups to bind to ice, and to see if there was a change in ice-binding with ionization state, 2 additional mutations of active residues were constructed (Q44E and N14D). Both mutants, in which amide groups were replaced by carboxyl groups, exhibited full activity at pH 3 and at pH 6. This surprising result showed that the 2 functional groups are equivalent in ice-binding, and that the strength of interaction is independent of the ionization state. Thus, asparagine, aspartate, and aspartic acid are roughly equivalent, as are glutamine, glutamate, and glutamic acid. Each set of functional groups has similar geometry but different H bond donor/acceptor properties overall, which were expected to cause differences in antifreeze activity. One partial explanation for the lack of pH sensitivity, as well as the unchanged activity for Q44E and N14D, is that the primary role of both the carboxyl and the amide groups is that of an H bond acceptor mediated through the carbonyl-oxygen.

Extent of the H bonding network

According to current models for the mechanism of action of macromolecular antifreezes (Wen & Laursen, 1992b; Knight et al., 1993), AFP and AFGP bind via an H bonding network to the ice surface in specific orientations and crystallographic adsorption planes. Despite the intrinsic weakness of some H bonds, it has been observed that AFPs with as few as 7 or 8 H bonding groups can hold an ice crystal without growth below the threshold supercooling temperature for an extended period of time (DeVries & Lin, 1977; Harrison et al., 1987). This has been our experience with wild-type QAE. It argues for the binding of AFPs to the ice surface to be virtually irreversible because ice is surrounded by 55 M H_2O. If there was a significant off-rate for the AFPs, then water would join the ice lattice very rapidly at the vacant surface sites leading to observable crystal growth.

In this study, only 3 residues were identified to be involved in H bonds with the ice surface. Two other polar residues on the C-terminal β-sheet were shown not to contribute to the H bond network between protein and ice. The replacement of asparagine by serine, which significantly reduced the AFP activity at position 14, was without effect at position 46 (N46S). It is possible that the side chain of N46 is sterically removed from the plane created by N14, T18, and Q44. Also, the side chain of S42 was shown by S42G not to be H bonded to the ice surface. This might have been expected in light of the sequence comparison of known Type III protein isoforms. From a structural viewpoint, however, the serine hydroxyl group is positioned approximately in the plane of the 3 active residues and is sterically capable of interacting with the ice surface. Thus, the result suggests a lack of a suitable H bond partner on the other side of the interface, the ice surface.

One polar residue of the C-terminal β-sheet not included in this study was T15. Although this residue is located within the framework of active residues, it is partially buried. All attempts at producing protein mutated at this position have failed so far, possibly due to folding problems. Thus, an interaction through its hydroxyl group is sterically unlikely but cannot be excluded at this time. Other additional protein-ice interactions could stem from the participation of backbone atoms in the H bond network. A16 and S42 backbone carbonyl oxygen atoms are partially surface accessible and sterically near the proposed site of interaction so that they might act as additional H bond accep-

tors to strengthen the overall protein–ice binding. However, these interactions are difficult to probe by mutagenesis.

Implications for current ice-binding models

Concerns about the number and strength of the bonds that hold AFP or AFGP onto the ice surface are central to a discussion of the mechanism of action of macromolecular antifreezes. As mentioned earlier, Knight et al. (1993) have addressed this issue by suggesting that some binding groups, such as -OH, can occupy positions in the ice lattice and thereby increase their number of H-bonds. Wen and Laursen (1992b) proposed a modified adsorption-inhibition mechanism. They argued that at low AFP concentrations or during early time points in the freezing trial, Type I AFPs bind reversibly to ice. This conclusion was based on regression analyses of early growth rate data (Wen & Laursen, 1992a). They suggested that AFP binding becomes irreversible only when AFPs form patches on the surface of ice through hydrophobic interpeptide interactions. It is the cooperative interaction between neighboring AFPs and the H-bonding between ice and protein that provide the total force needed to prevent ice growth (Wen & Laursen, 1992b).

It is not clear that the action of Type III AFP can be adequately explained by the latter model. In the ocean pout, there are multiple AFP isoforms that are independently active (Li et al., 1985). Although they probably all have the same globular fold (Chao et al., 1993), they are different enough in amino acid sequence to make it unlikely that they could substitute for each other in the cooperative binding network necessary to form an AFP patch. However, if the patches are homogeneous, then the presence of similar isoforms in high concentrations should competitively inhibit patch formation.

Specific ice-adsorption planes have been determined for Type I AFP and AFGP. Even after identification of the ice-binding residues of Type III AFP, the issue of whether or not there are discrete adsorption planes for this globular antifreeze remains unresolved. The residues involved are not regularly spaced and are of different character, so that an identification of possible adsorption planes at the current resolution of the NMR structure is not feasible. Also, with the implied presence of additional, though as yet unidentified, interacting groups, it is questionable whether all the groups are located in 1 plane. Given the lack of repetitive character, the irregular backbone structure of this AFP, and the demonstrated importance of structurally diverse active groups, it is quite possible that the adsorption site cannot be correlated with specific crystallographic planes. Moreover, with the significantly smaller dimensions (length) of the interface (16 Å versus 50 Å for Type I AFP) only few, low-order crystallographic planes are accessible to this protein.

Without the restriction of adsorption to a specific plane, one could hypothesize that after initial, low-affinity attachment to the ice surface (for which H-bonding residues T18, N14, and Q44 are responsible), the ice continues to grow in the vicinity of the protein and "anchors" it to the surface. That is to say, the protein is partially included into the ice. Under these circumstances, additional polar residues near the C-terminal β-sheet (at the sides of the protein) could also interact with the interface, as might some amide and carbonyl groups of the polypeptide backbone. For this type of interaction, the globular fold of Type III AFP might actually be advantageous. In particular, with a diameter of approximately 20 Å, even a partially buried protein would protrude well beyond the ice–water interface. Thus, the chances of the protein being completely enclosed in the ice lattice are negligible at sufficiently high protein concentrations. This hypothesis is also compatible with the implied rigidity of the ice–AFP interface and the proposed residue-specific adsorption sites. Additional mutations of polar or other residues in the wider vicinity of the C-terminal β-sheet might allow us to probe the distance between these regions and the ice–water interface and provide experimental evidence for further evaluation of this hypothesis. These studies are currently underway in our laboratory.

Materials and methods

Production and purification of recombinant AFP

Production of recombinant Type III AFP (rQAE m1.1) and its mutants from a synthetic gene was done as previously described (Chao et al., 1993) with the following modifications. The Triton X-100-washed inclusion body pellet from a 3-L culture was resuspended in 8–10 mL of 8 M guanidine-HCl, 100 mM Tris-HCl (pH 8.5) with gentle mixing at 20 °C for 1 h. It was then added dropwise to 160 mL of ice-cold refolding buffer containing 50 mM K_2HPO_4 and 100 mM NaCl (pH 10.7). The sample was left to stir gently on ice for an additional 30 min. This mixture was dialyzed against 50 mM sodium acetate (pH 3.7) at 4 °C. After clarification by centrifugation, the supernatant was applied to an S-Sepharose FPLC column (Pharmacia) and Type III AFP was isolated as before (Chao et al., 1993).

Primer-directed mutagenesis

Mutants N14S, N14D, N14Q, T18S, T18N, S42G, Q44T, Q44E, and N46S were made by primer-directed mutagenesis (Kunkel et al., 1987) as described previously (Chao et al., 1993). The mutagenic oligonucleotides used are listed in Figure 1. In addition to the use of plasmid pTZ-19r (Mead et al., 1986) for the generation of single-stranded, uracil-containing template, a second plasmid pT7-7(f) was also used. pT7-7(f) was made by the incorporation of an f1 origin of replication into the expression vector pT7-7 (Tabor, 1990) as previously described (DeLuca et al., 1993). This allowed Kunkel's method of mutagenesis to be done directly on the expression vector.

Double and triple mutants

Mutant N14S/Q44T was made by splicing together DNA from mutants N14S and Q44T. The *Nde* I/*Eco* RV fragment from mutant plasmid N14S and the *Eco* RV/*Eco* RI fragment from mutant plasmid Q44T were gel purified and ligated into *Nde* I/*Eco* RI-cut pT7-7. Ligated products were transformed into *Escherichia coli* K38 cells. Mutants were identified by double-stranded dideoxy sequencing. The triple mutant N14S/T18N/Q44T was constructed by primer-directed mutagenesis on template generated from the double mutant N14S/Q44T.

Analysis of AFP mutants

Thermal hysteresis was used as a measure of antifreeze activity. Thermal hysteresis is defined as the difference between so-

lution freezing and melting temperatures. All measurements (except for the pH dependence study below) were made in 100 mM NH_4HCO_3 (pH 7.9) using a nanoliter osmometer (Clifton Technical Physics, Hartford, New York) as described by Chakrabartty et al. (1991).

pH dependence study

The antifreeze activity of rQAE m1.1 (1.0 mg/mL) was measured at pH values ranging from 1 to 13. For samples within the pH 2–11 range, an aliquot of rQAE m1.1 (4 mg/mL) was added to a pH-adjusted buffer mixture of 100 mM sodium citrate, 100 mM sodium phosphate, and 100 mM sodium borate. After minor pH adjustment with either 1 N NaOH or 1 N HCl, deionized water was added so that the final concentration of protein was 1.0 mg/mL and the final concentration of each of the buffers was 50 mM. For pH 1, thermal hysteresis of rQAE m1.1 was measured in 100 mM HCl and 150 mM NaCl. For pH 13, measurements were taken in 100 mM NaOH and 50 mM NaCl.

The antifreeze activity of N14D (1 mg/mL) and Q44E (1 mg/mL) was measured at pH 3 and at pH 6 in the same buffer system used for rQAE m1.1.

NMR experiments

All experiments were carried out on 0.5-mL samples in a Varian Unity 500 spectrometer at a ^1H frequency of 500 MHz. One to four mg of each AFP was dissolved in 100% D_2O to yield 0.2–0.8 mM solutions. All spectra were acquired at 3 °C with pH values adjusted to 7.0 (not corrected for deuterium isotope effects). One-dimensional spectra were acquired using 24,000 data points, a spectral width of 7,500 Hz, 2,048 transients with 1.4–2.0-s presaturation delay, and a 90° pulse width of 10 μs. The data were processed with 0 filling to 64K points and with exponential line broadening of 0.5–1.5 Hz. Two-dimensional experiments for rQAE m1.1 and Q44T were acquired in the phase-sensitive mode using the methods of States et al. (1982), using 300 t_1 increments, 32–64 scans per increment, and 2,048 data points per scan with a spectral width of 7,500 Hz. DQF-COSY spectra (Piantini et al., 1982; Rance et al., 1983), NOESY spectra with mixing times of 100 ms (Jeener et al., 1979; Kumar et al., 1980; Macura et al., 1981), and TOCSY spectra (Braunschweiler & Ernst, 1983; Davis & Bax, 1985) were acquired, the latter using isotropic mixing times of 60 ms and an MLEV-17 pulse sequence (Davis & Bax, 1985) to produce a spin lock field of 7.3 kHz. The 2D data were processed on a SUN-IPC workstation using the Varian VNMR software package. Routinely, the data were 0 filled to 4K × 4K data points and shifted sinebells were used for resolution enhancement in both dimensions.

Acknowledgments

We thank Sherry Gauthier and Gerry McQuaid for technical assistance. This work was supported by research grants from the Medical Research Council of Canada (B.D.S., P.L.D.). the Protein Engineering Network of Centres of Excellence (B.D.S., F.D.S.), and the Alberta Heritage Foundation for Medical Research (F.D.S.). H.C. was the recipient of an Ontario Graduate Scholarship and C.I.D. and was supported by a Medical Research Council Studentship. P.L.D. dedicates this paper to Dr. Michael Smith, recipient of the 1993 Nobel Prize for Chemistry, for his pioneering work on site-directed mutagenesis.

References

Braunschweiler L, Ernst RR. 1983. Coherence transfer by isotropic mixing: Application to proton correlation spectroscopy. *J Magn Reson 53*:521–528.

Chakrabartty A, Hew CL. 1991. The effect of enhanced α-helicity on the activity of a winter flounder antifreeze polypeptide. *Eur J Biochem 202*:1057–1063.

Chao H, Davies PL, Sykes BD, Sönnichsen FD. 1993. Use of proline mutants to help solve the NMR solution structure of type III antifreeze protein. *Protein Sci 2*:1411–1428.

Davies PL, Hew CL. 1990. Biochemistry of fish antifreeze proteins. *FASEB J 4*:2460–2468.

Davis DG, Bax A. 1985. Assignment of complex ^1H NMR spectra via two-dimensional homonuclear Hartmann-Hahn spectroscopy. *J Am Chem Soc 107*:2820–2821.

DeLuca CI, Davies PL, Samis JA, Elce JS. 1993. Molecular cloning and bacterial expression of cDNA for rat calpain II 80 kDa subunit. *Biochim Biophys Acta 1216*:81–93.

DeVries AL. 1983. Antifreeze peptides and glycopeptides in coldwater fishes. *Annu Rev Physiol 45*:245–260.

DeVries AL. 1984. Role of glycopeptides and peptides in inhibition of crystallization of water in polar fishes. *Philos Trans R Soc Lond B Biol Sci B 304*:575–588.

DeVries AL, Lin Y. 1977. The role of glycopeptide antifreezes in the survival of Antarctic fishes. In: Liano GA, ed. *Adaptations within Antarctic ecosystems: Proceedings of the third SCAR symposium on Antarctic biology*. Houston, Texas: Gulf Publishing Co. pp 439–458.

Harrison K, Hallett J, Burcham TS, Feeney RE, Kerr WL, Yeh Y. 1987. Ice growth in supercooled solutions of antifreeze glycoprotein. *Nature 328*:241–243.

Jeener J, Meier BH, Bachmann P, Ernst RR. 1979. Investigation of exchange processes by two-dimensional NMR spectroscopy. *J Chem Phys 71*: 4546–4553.

Kim KS, Woodward C. 1993. Protein internal flexibility and global stability: Effect of urea on hydrogen exchange rates of bovine pancreatic trypsin inhibitor. *Biochemistry 32*:9609– 9613.

Knight CA, Cheng CC, DeVries AL. 1991. Adsorption of α-helical antifreeze peptides on specific ice crystal surface planes. *Biophys J 59*:409–418.

Knight CA, Driggers E, DeVries AL. 1993. Adsorption to ice of fish antifreeze glycopeptides. *Biophys J 64*:252–259.

Kumar A, Ernst RR, Wüthrich K. 1980. A two-dimensional nuclear Overhauser enhancement (2D NOE) experiment for the elucidation of complete proton-proton relaxation networks in biological macromolecules. *Biophys Res Commun 95*:1–6.

Kunkel TA, Roberts JD, Zarkour RA. 1987. Rapid and efficient site-specific mutagenesis without phenotypic selection. *Methods Enzymol 154*:367–382.

Li XM, Trinh KY, Hew CL, Buettner B, Baenziger J, Davies PL. 1985. Structure of an antifreeze polypeptide and its precursor from the ocean pout, *Macrozoarces americanus*. *J Biol Chem 260*:12902–12909.

Macura S, Huong Y, Suter D, Ernst RR. 1981. Two-dimensional chemical exchange and cross-relaxation spectroscopy of coupled nuclear spins. *J Magn Reson 43*:259–281.

Madura JD, Wierzbicki A, Harrington JP, Maughon RH, Raymond JA, Sikes CS. 1994. Interactions of the D- and L-forms of winter flounder antifreeze peptide with the {201} planes of ice. *J Am Chem Soc 116*: 417–418.

Mead DA, Szczesna-Skorupa E, Kemper B. 1986. Single-stranded DNA "blue" T7 promoter plasmids: A versatile tandem promotor system for cloning and protein engineering. *Protein Eng 1*:67–74.

Piantini U, Sørensen OW, Ernst RR. 1982. Multiple quantum filters for elucidating NMR coupling networks. *J Am Chem Soc 104*:6800–6801.

Rance M, Sørensen OW, Bodenhausen G, Wagner G, Ernst RR, Wüthrich K. 1983. Improved spectral resolution in COSY ^1H NMR spectra of proteins via double quantum filtering. *Biochem Biophys Res Commun 117*:479–485.

Raymond JA, DeVries AL. 1977. Adsorption inhibition as a mechanism of freezing resistance in polar fishes. *Proc Natl Acad Sci USA 74*:2589–2593.

Shrake A, Rupley JA. 1973. Environment and exposure to solvent of protein atoms. Lysozyme and insulin. *J Mol Biol 79*:351–371.

Sönnichsen FD, Sykes BD, Chao H, Davies PL. 1993. The nonhelical structure of antifreeze protein type III. *Science 259*:1154–1157.

States DJ, Haberkorn RA, Ruben DJ. 1982. A two-dimensional nuclear Over-

hauser experiment with pure absorption phase in four quadrants. *J Magn Reson 48*:296–292.

Tabor S. 1990. Expression using the T7 RNA polymerase/promoter system. In: Ausubel FA, Brent R, Kingston RE, Moore DD, Seidman JG, Smith JA, Struhl K, eds. *Current protocols in molecular biology*. New York: Greene Publishing and Wiley-Interscience. pp 16.2.1–16.2.11.

Wen D, Laursen RA. 1992a. Structure-function relationships in an antifreeze polypeptide. *J Biol Chem 267*:14102–14108.

Wen D, Laursen RA. 1992b. A model for binding of an antifreeze polypeptide to ice. *Biophys J 63*:1659–1671.

Wishart DS, Sykes BD, Richards FM. 1991. Relationship between nuclear magnetic resonance chemical shift and protein secondary structure. *J Mol Biol 222*:311–333.

Yang DSC, Sax M, Chakrabartty A, Hew CL. 1988. Crystal structure of an antifreeze polypeptide and its mechanistic implications. *Nature 333*: 232–237.